Funct Integr Genomics (2011) 11:225–239
DOI 10.1007/s10142-011-0210-y

ORIGINAL PAPER

Mitochondrial proteomics analysis of tumorigenic and metastatic breast cancer markers

Yi-Wen Chen · Hsiu-Chuan Chou · Ping-Chiang Lyu · Hsien-Sheng Yin · Fang-Liang Huang · Wun-Shaing Wayne Chang · Chiao-Yuan Fan · I-Fan Tu · Tzu-Chia Lai · Szu-Ting Lin · Ying-Chieh Lu · Chieh-Lin Wu · Shun-Hong Huang · Hong-Lin Chan

Received: 30 October 2010 / Revised: 2 January 2011 / Accepted: 4 January 2011 / Published online: 19 January 2011

Abstract Mitochondria are key organelles in mammary cells responsible for several cellular functions including growth, division, and energy metabolism. In this study, mitochondrial proteins were enriched for proteomics analysis with the state-of-the-art two-dimensional differential gel electrophoresis and matrix-assistant laser desorption ionization–time-of-flight mass spectrometry strategy to compare and identify the mitochondrial protein profiling changes between three breast cell lines with different tumorigenicity and metastasis. The proteomics results demonstrate more than 1,500 protein features were resolved from the equal amount pooled from three purified mitochondrial proteins, and 125 differentially expressed spots were identified by their peptide finger print, in which, 33 identified proteins belonged to mitochondrial proteins. Eighteen out of these 33 identified mitochondrial proteins such as SCaMC-1 have not been reported in breast cancer research to our knowledge. Additionally, mitochondrial protein prohibitin has shown to be differentially distributed in mitochondria and in nucleus for normal breast cells and breast cancer cell lines, respectively. To sum up, our approach to identify the mitochondrial proteins in various stages of breast cancer progression and the identified proteins may be further evaluated as potential breast cancer markers in prognosis and therapy.

Keywords Breast cancer · Biomarker · Proteomics · Mitochondria · DIGE · MALDI-TOF · Tumorigenesis · Metastasis · Prohibitin · SCaMC-1

Abbreviations

1-DE	One-dimensional gel electrophoresis
2-DE	Two-dimensional gel electrophoresis
Ab	Antibody
CCB	Colloidal Coomassie blue
CHAPS	3-[(3-Cholamidopropyl)-dimethylammonio]-1-propanesulfonate)
ddH_2O	Double deionized water

Electronic supplementary material The online version of this article (doi:10.1007/s10142-011-0210-y) contains supplementary material, which is available to authorized users.

Y.-W. Chen · P.-C. Lyu · H.-S. Yin · C.-Y. Fan · I.-F. Tu · T.-C. Lai · S.-T. Lin · Y.-C. Lu · C.-L. Wu · S.-H. Huang · H.-L. Chan (✉)
Institute of Bioinformatics and Structural Biology and Department of Medical Sciences, National Tsing Hua University, No. 101, Kuang-Fu Rd. Sec. 2, Hsinchu 30013, Taiwan
e-mail: hlchan@life.nthu.edu.tw

H.-C. Chou
Department of Applied Science, National Hsinchu University of Education, Hsinchu, Taiwan

F.-L. Huang
Pediatric Department, Taichung Veterans General Hospital, Taichung, Taiwan

W.-S. W. Chang
National Institute of Cancer Research, National Health Research Institutes, Zhunan Town, Miaoli 350, Taiwan

DIGE	Differential gel electrophoresis
DTT	Dithiothreitol
FCS	Fetal calf serum
MALDI-TOF MS	Matrix-assisted laser desorption ionization–time-of-flight mass spectrometry
NP-40	Nonidet P-40
TFA	Trifluoroacetic acid

Introduction

Breast cancer is one of the leading causes of death among women in the world. Previous studies have shown that the transformation and metastasis of normal breast cells are both correlated to the altered expression in transcriptional level and translational level (Hondermarck et al. 2002; Kulasingam and Diamandis, 2007; Lee et al. 2007; Morrow 2007; Nuyten and van de Vijver 2008). Proteomics strategies have been used to discover the cancer markers from non-invasive and invasive breast cells. Nagaraja et al. compared the proteomic profiling of cell lines corresponding to normal breast cell, non-invasive breast cancer, and invasive breast cancer by two-dimensional gel electrophoresis (2-DE) (Nagaraja et al. 2006). Pucci-Minafra et al. compared a ductal infiltrating carcinoma-derived cell line with a non-tumoral mammary epithelial cell line by 2-DE, silver stain, immunodetection, and N-terminal sequencing and finally identified 58 differentially expressed proteins (Pucci-Minafra et al. 2002).

The main function of mitochondria is to produce cellular energy by breaking down lipids and glucose to form acetyl-coenzyme A which can pass through the Kreb's cycle and respiratory chain to generate ATP (von Jagow and Engel 1980). Accordingly, mitochondria are essential for the survival of eukaryotic cells, and mitochondrial defects contribute to the development of numerous human diseases including cancer (Taylor and Turnbull 2005). Since the initial publications of Warburg's hypothesis, nearly a half century of scientific researches believed that mitochondrial damage is one of the most common characteristics of cancer cells, and mitochondrial deregulation plays a key role to trigger tumorigenesis and metastasis (Gogvadze et al. 2008). For example, the subcellular distribution of human mitochondrial mortalin has been shown to significantly associate with aggressive cancers in a variety of human cancer cell lines (Wadhwa et al. 1993a). Elevated level of mortalin expression in cytoplasmic fraction is able to sequester the tumor suppressor protein p53 and activates the *Ras–Raf* signaling pathway, which exerts the deregulation of cell growth and eventually formation of malignancies (Wadhwa et al. 2002a; Wadhwa et al. 2003a). In addition, hypoxia-inducing factor 1 (HIF-1) is an activator of a number of genes whose products are implicated in crucial aspects of cancer biology, including angiogenesis (Pouyssegur et al. 2006), epithelial–mesenchymal transition (Esteban et al. 2006), cancer metastasis (Chi et al. 2007), as well as the activation of matrix metalloprotease (Kumar et al. 2008). Since mitochondrial respiratory complex III has been reported to regulate the hypoxic stabilization of HIF-1 (Chandel et al. 2000), it is directly involved in the impairment of important cancer regulators and mediates the generation of cancers. Taken together, these examples support the notion that the alteration of mitochondria contributes to the tumorigenic, invasive, angiogenetic, and metastatic features of cancer cells.

2-DE is currently a key technique in profiling thousands of proteins within biological samples and plays a complementary role to LC/MS-based (liquid chromatography/mass spectrometry) proteomic analysis (Timms and Cramer 2008). However, reliable quantitative comparisons between gels and gel-to-gel variations remain the primary challenge in 2-DE analysis. A significant improvement in the gel-based analysis of protein quantitation and detection was achieved by the introduction of two-dimensional differential gel electrophoresis (2D-DIGE), which can co-detect numerous samples in the same 2-DE. This approach minimizes gel-to-gel variations and compares the relative amount of protein features across different gels using an internal fluorescent standard. Moreover, the 2D-DIGE technique has the advantages of a broader dynamic range, higher sensitivity, and greater reproducibility than traditional 2-DE. This innovative technology relies on the pre-labeling of protein samples with fluorescent dyes (Cy2, Cy3, and Cy5) before electrophoresis. Each dye has a distinct fluorescent wavelength, allowing multiple experimental samples with an internal standard to be simultaneously separated in the same gel. The internal standard, which is a pool of an equal amount of the experimental protein samples, helps provide accurate normalization data and increase statistical confidence in relative quantitation among gels (Chan et al. 2005;Chan et al. 2006;Lai et al. 2010;Chou et al. 2010; Huang et al. 2010).

In order to thoroughly understand the molecular mechanisms associated with tumorigenesis and metastasis, it is necessary to identify the low-abundant cancer markers as well as to identify the high- and middle-abundant markers across normal breast cells, non-invasive breast cancers, and invasive breast cancers. In this study, we have purified mitochondrial proteins from three breast cells, MCF10A, MCF7, and MDA-MB-231, corresponding to normal luminal epithelial cells, the non-invasive breast cancer cells derived from luminal duct, and invasive breast cancer cells derived from the same tissues, respectively, followed by quantitatively identified potential mitochondrial transformation markers of breast cancer by 2D-DIGE and MALDI-TOF mass spectrometry.

Materials and methods

Chemical and reagents

Generic chemicals were purchased from Sigma-Aldrich (St. Louis, USA), while reagents for 2D-DIGE were purchased from GE Healthcare (Uppsala, Sweden). All primary antibodies were purchased from Abcam (Cambridge, UK), and anti-mouse, anti-goat, and anti-rabbit secondary antibodies were purchased from GE Healthcare (Uppsala, Sweden). All the chemicals and biochemicals used in this study were of analytical grade.

Cell lines and cell culture

The breast epithelial cell line MCF-10A was a gift from Dr. Wun-Shaing Wayne Chang, National Health Research Institute, Taiwan. The breast cancer cell lines MCF-7 (non-invasive), MDA-MB-231 (invasive), MDA-MB-453 (non-invasive), MDA-MB-361 (invasive), MDA-MB-435 (invasive), and SKBR3 (invasive) were purchased from American Type Culture Collection, Manassas, VA. MCF-10A was maintained in Dulbecco's Modified Eagle's medium and F-12 medium supplemented with 5% horse serum, L-glutamine (2 mM), streptomycin (100 μg/ml), penicillin (100 IU/ml), epidermal growth factor (20 ng/ml; all from Gibco-Invitrogen Corp., UK), insulin (10 μg/ml; Sigma), and hydrocortisone (0.5 μg/ml; Sigma). MCF-7, MDA-MB-231, MDA-MB-453, MDA-MB-361 MDA-MB-435, and SKBR3 were maintained in Dulbecco's Modified Eagle's medium supplemented with 10% (*v*/*v*) FCS, L-glutamine (2 mM), streptomycin (100 μg/mL), and penicillin (100 IU/mL; all from Gibco-Invitrogen Corp., UK). All cells were incubated at 37°C and 5% CO_2.

Sample preparation for proteomic analysis

Mitochondria were isolated using the mitochondrial isolation kit for mammalian cells (Pierce) according to the manufacturer's instructions, with some modifications. Briefly, following lysis of approximately 2.5×10^7 of MCF-10A, MCF-7, or MDA-MB-231, cell debris and nuclei were pelleted at 700×*g*, followed by centrifugation at 5,000×*g* to pellet a mitochondrially enriched fraction. The crude mitochondria were washed in chilled 0.5× phosphate-buffered saline (PBS) and lysed in 2-DE lysis buffer containing 4% *w*/*v* CHAPS, 7 M urea, 2 M thiourea, 10 mM Tris–HCl, pH 8.3, 1 mM EDTA (ethylenediaminetetraacetic acid). Lysates were homogenized by passage through a 25-gauge needle for ten times and the insoluble material removed by centrifugation at 13,000 rpm for 30 min at 4°C, and protein concentrations were determined using the Coomassie protein assay reagent (BioRad).

2D-DIGE and gel image analysis

Before performing 2D-DIGE, protein samples were labeled with *N*-hydroxy succinimidyl ester-derivatives of the cyanine dyes Cy2, Cy3, and Cy5 following the protocol described previously (Gharbi et al. 2002; Chan et al. 2005; Lai et al. 2010). Briefly, 150 μg of protein sample was minimally labeled with 375 pmol of either Cy3 or Cy5 for comparison on the same 2-DE. To facilitate image matching and cross-gel statistical comparison, a pool of all samples was also prepared and labeled with Cy2 at a molar ratio of 2.5 pmol Cy2 per μg of protein as an internal standard for all gels. Thus, the triplicate samples and the internal standard could be run and quantified on multiple 2-DE. The labeling reactions were performed in the dark on ice for 30 min and then quenched with a 20-fold molar ratio excess of free L-lysine to dye for 10 min. The differentially Cy3- and Cy5-labeled samples were then mixed with the Cy2-labeled internal standard and reduced with dithiothreitol for 10 min. IPG buffer, pH 3–10 non-linear [2% (*v*/*v*), GE Healthcare] was added, and the final volume was adjusted to 450 μl with 2D-lysis buffer for rehydration. The rehydration process was performed with immobilized non-linear pH gradient (IPG) strips (pH 3–10, 24 cm) which were later rehydrated by CyDye-labeled samples in the dark at room temperature overnight (at least 12 h). Isoelectric focusing was then performed using a Multiphor II apparatus (GE Healthcare) for a total of 62.5 kV-h at 20°C. Strips were equilibrated in 6 M urea, 30% (*v*/*v*) glycerol, 1% SDS (sodium dodecyl sulfate) (*w*/*v*), 100 mM Tris–HCl (pH 8.8), 65 mM dithiothreitol for 15 min, and then in the same buffer containing 240 mM iodoacetamide for another 15 min. The equilibrated IPG strips were transferred onto 26×20 cm 12.5% polyacrylamide gels casted between low fluorescent glass plates. The strips were overlaid with 0.5% (*w*/*v*) low melting point agarose in a running buffer containing bromophenol blue. The gels were run in an Ettan Twelve gel tank (GE Healthcare) at 4 Watts per gel at 10°C until the dye front had completely run off the bottom of the gels. Afterward, the fluorescence 2-DE was scanned directly between the low fluorescent glass plates using an Ettan DIGE Imager (GE Healthcare). This imager is a charge-coupled device-based instrument that enables scanning at different wavelengths for Cy2-, Cy3-, and Cy5-labeled samples. Gel analysis was performed using DeCyder 2-D Differential Analysis Software v7.0 (GE Healthcare) to co-detect, normalize, and quantify the protein features in the images. Features detected from non-protein sources (e.g., dust particles and dirty backgrounds) were filtered out. Spots displaying a ≥1.5 average-fold increase or decrease in abundance with a p value<0.05 were selected for protein identification.

Protein staining

Colloidal Coomassie blue G-250 staining was used to visualize CyDye-labeled protein features in 2-DE. Bonded gels were fixed in 30% *v*/*v* ethanol, 2% *v*/*v* phosphoric acid overnight, washed three times (30 min each) with ddH_2O and then incubated in 34% *v*/*v* methanol, 17% *w*/*v* ammonium sulfate, 3% *v*/*v* phosphoric acid for 1 h, prior to adding 0.5 g/l Coomassie blue G-250. The gels were then left to stain for 5–7 days. No destaining step was required. The stained gels were then imaged on an Image-Scanner III densitometer (GE Healthcare), which processed the gel images as .tif files.

In-gel digestion

Excised post-stained gel pieces were washed three times in 50% acetonitrile, dried in a SpeedVac for 20 min, reduced with 10 mM dithiothreitol in 5 mM ammonium bicarbonate pH 8. 0 (ammonium bicarbonate) for 45 min at 50°C, and then alkylated with 50 mM iodoacetamide in 5 mM bicarbonate for 1 h at room temperature in the dark. The gel pieces were then washed three times in 50% acetonitrile and vacuum-dried before reswelling with 50 ng of modified trypsin (Promega) in 5 mM ammonium bicarbonate. The pieces were then overlaid with 10 μl of 5 mM ammonium bicarbonate and trypsinized for 16 h at 37°C. Supernatants were collected; peptides were further extracted twice with 5% trifluoroacetic acid in 50% acetonitrile, and the supernatants were pooled. Peptide extracts were vacuum-dried, resuspended in 5 μl ddH_2O, and stored at −20°C prior to mass spectrometry analysis.

Protein identification by MALDI-TOF MS

Extracted proteins were cleaved with a proteolytic enzyme to generate peptides and then a peptide mass fingerprinting database search following MALDI-TOF MS was employed for protein identification. Briefly, 0.5 μl of tryptic digested protein sample was first mixed with 0.5 μl of a matrix solution containing α-cyano-4-hydroxycinammic acid at a concentration of 1 mg in 1 ml of 50% acetonitrile (*v*/*v*)/0.1% trifluoroacetic acid (*v*/*v*), spotted onto an anchorchip target plate (Bruker Daltonics), and dried. The peptide mass fingerprints were acquired using an Autoflex III mass spectrometer (Bruker Daltonics) in reflector mode. The algorithm used for spectrum annotation was SNAP (Sophisticated Numerical Annotation Procedure). This process used the following detailed metrics: peak detection algorithm, SNAP; signal-to-noise threshold, 25; relative intensity threshold, 0%; minimum-intensity threshold, 0; maximal number of peaks, 50; quality factor threshold, 1,000; SNAP average composition, averaging; baseline subtraction, median; flatness, 0.8; median level, 0.5. The spectrometer was also calibrated with a peptide calibration standard (Bruker Daltonics), and internal calibration was performed using trypsin autolysis peaks at *m/z* 842.51 and *m/z* 2211.10. Peaks in the mass range of *m/z* 800–3,000 were used to generate a peptide mass fingerprint that was searched against the Swiss-Prot/TrEMBL database (v57.12) with 513,877 entries using Mascot software v2.2.06 (Matrix Science, London, UK). The following parameters were used for the search: *Homo sapiens*; tryptic digest with a maximum of one missed cleavage; carbamidomethylation of cysteine, partial protein N-terminal acetylation, partial methionine oxidation and partial modification of glutamine to pyroglutamate, and a mass tolerance of 50 ppm. Identification was accepted based on significant MASCOT Mowse scores ($p<0.05$), spectrum annotation, and observed versus expected molecular weight and p*I* on 2-DE.

Immunoblotting

Immunoblotting was used to validate the differential expression of mass spectrometry-identified proteins. Cells were lysed with a lysis buffer containing 50 mM HEPES pH 7.4, 150 mM NaCl, 1% NP40, 1 mM EDTA, 2 mM sodium orthovanadate, 100 μg/mL AEBSF, 17 μg/mL aprotinin, 1 μg/mL leupeptin, 1 μg/mL pepstatin, 5 μM fenvalerate, 5 μM BpVphen, and 1 μM okadaic acid prior to protein quantification with Coomassie Protein Assay Reagent (BioRad). Thirty micrograms of of protein samples were diluted in Laemmli sample buffer [final concentrations, 50 mM Tris, pH 6.8, 10% (*v*/*v*) glycerol, 2% SDS (*w*/*v*), 0.01% (*w*/*v*) bromophenol blue] and separated by 1D-SDS-PAGE following standard procedures. After electroblotting separated proteins onto 0.45 μm Immobilon P membranes (Millipore), the membranes were blocked with 5% *w*/*v* skim milk in TBS-T (50 mM Tris pH 8.0, 150 mM NaCl, and 0.1% Tween-20 (*v*/*v*)) for 1 h. Membranes were then incubated in primary antibody solution in TBS-T containing 0.02% (*w*/*v*) sodium azide for 2 h. Membranes were washed in TBS-T (3×10 min) and then probed with the appropriate horseradish peroxidase-coupled secondary antibody (GE Healthcare). After further washing in TBS-T, immunoprobed proteins were visualized using an enhanced chemiluminescence method (Visual Protein Co).

Immunofluorescence

For immunofluorescence staining, cells were plated onto coverslips (VWR international) for overnight incubation. The cells were fixed with PBS containing 4% (*v*/*v*) paraformaldehyde for 25 min, washed three times with PBS, and followed by permeabilization in PBS containing 0.2% (*v*/*v*) Triton X-100 for 10 min. Coverslips were rinsed

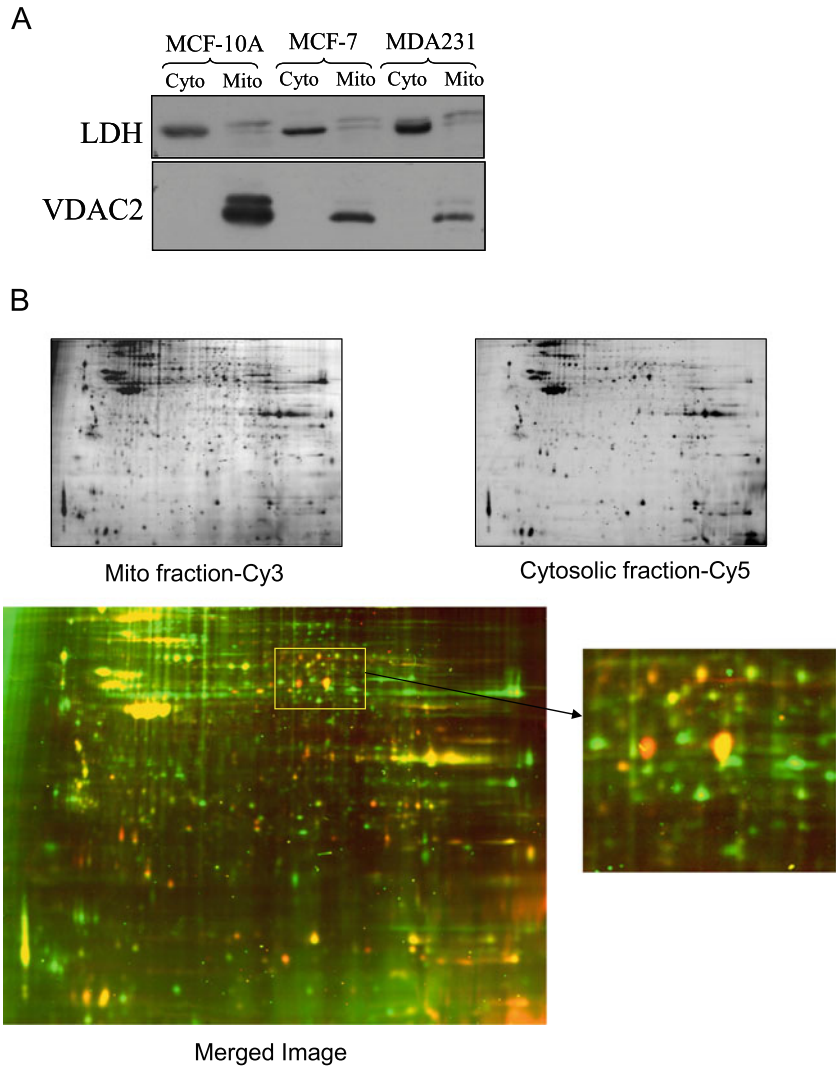

Fig. 1 Analysis of purity of the mitochondrial protein extracts by immunoblotting and 2D-DIGE. Mitochondrial and cytosolic fractions were prepared from MCF-10A, MCF-7, and MDA-MB-231 cells. Purity of both fractions was determined by immunoblotting analysis using antibodies against cytoplasmic localized marker protein: LDH and a mitochondrial localized marker protein: VDAC 2 (**a**). Protein samples (50 μg each) purified from mitochondrial and cytosolic fractions of MCF-7 cells were labeled with Cy3- and Cy5-dyes, respectively, and separated using 24 cm, pH 3–10 non-linear IPG strips followed by resolved with 12.5% SDS-PAGE. 2D-DIGE images of Cy3- and Cy5-labeled proteins at appropriate excitation and emission wavelengths were pseudo-colored and overlaid with ImageQuant Tool (GE Healthcare) (**b**)

and blocked in PBS containing 5% (*w*/*v*) BSA (bovine serum albumin) for 10 min before incubation with primary antibodies diluted in 2.5% BSA/PBS (bovine serum albumin in phosphate buffered saline) for 1 hr. After three washings with PBS, samples were incubated with the appropriate fluorescently labeled secondary antibodies diluted in 2.5% BSA/PBS for 1 h. Coverslips were then washed three times with PBS and at least twice with ddH_2O before mounting in Vectashield mounting medium (Vector Lab). Coverslip edges were sealed with nail polish onto glass slides (BDH) and then dried in the dark at 4°C. For image analysis, cells were imaged using a Zeiss Axiovert 200 M fluorescent microscope (Carl Zeiss Inc., Germany). The laser intensities used to detect the same immunostained markers from different cell lines were identical, and none of the laser intensities used to capture images was saturated. Images were exported as .tif files using the Zeiss Axioversion 4.0 and processed using Adobe Photoshop V.7.0 software. For the study of mitochondrial location, living cells were incubated with MitoTracker Orange CM-H_2TMRos (100 nM, 20 min, Invitrogen) at 37°C, and washed in PBS. MitoTracker-loaded cells were then fixed in 4% paraformaldehyde and rinsed with PBS for 10 min. Cells were permeabilization in PBS containing 0.2% (*v*/*v*) Triton X-100 for 10 min and then blocked in PBS/1% BSA for 1 h.

Enzyme-linked immunosorbent assay analysis of plasma

After informed consent was given; plasma were obtained from five healthy individuals used as the control, five breast cancer patients without detectable metastasis, and five breast cancer patients presenting metastasis at the time of serum collection. All of plasma were from a single center and were enrolled in the study. Enzyme-linked immunosorbent assay (ELISA) was used to validate the differential expression of SCaMC-1. Briefly, EIA polystyrene microtitration wells were coated with 50 μg of plasma samples and incubated at 37°C for 2 h. The plate was washed for three times with phosphate-buffered saline–Tween 20 (PBST) and three times with

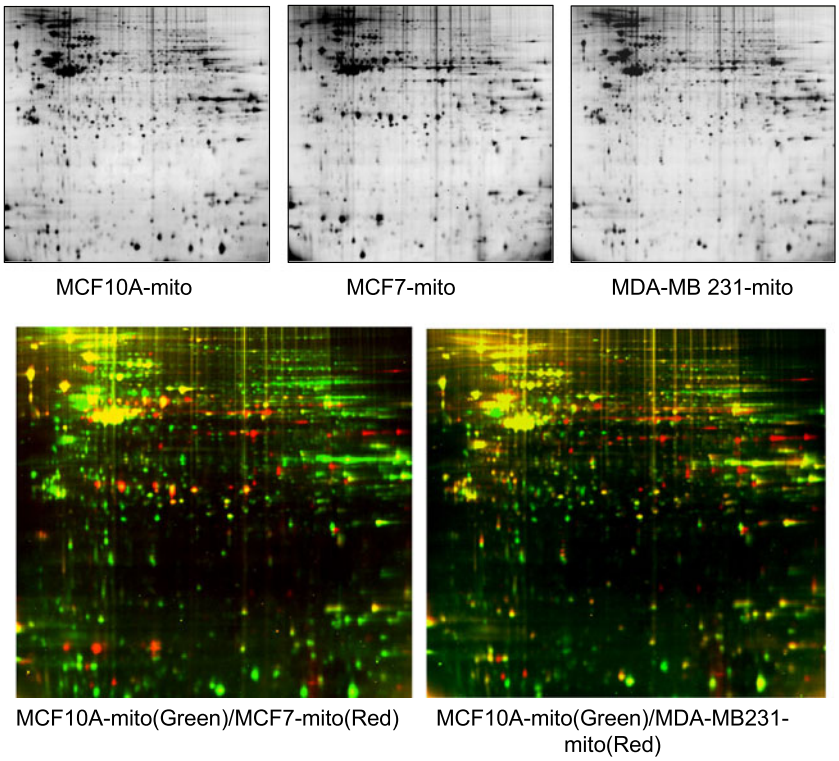

Fig. 2 Analysis of the breast mitochondrial proteomes of MCF-10A, MCF-7, and MDA-MB-231 cells by 2D-DIGE. Mitochondrial proteins (50 μg each) purified from MCF-10A, MCF-7, and MDA-MB-231 cells were labeled with Cy-dyes and separated using 24 cm, pH 3–10 non-linear IPG strips followed by resolved with 12.5% SDS-PAGE. 2D-DIGE images of MCF-10A, MCF-7, and MDA-MB-231 at appropriate excitation and emission wavelengths were pseudo-colored and overlaid with ImageQuant Tool (GE Healthcare)

PBS. After the uncoated space was blocked with 100 μl of 5% skimmed milk in PBS at 37°C for 2 h, the plate was washed three times with PBST. SCaMC-1 antibody (Abcam) solution was added and incubated at 37°C for 2 h. After washing with PBST and PBS for ten times in total, 100 μl of peroxidase-conjugated secondary antibodies in PBS was added for incubation at 37°C for 2 h. Following ten washings, 100 μl of 3,3',5,5'-tetramethyl benzidine (Pierce) was added. After incubation at room temperature for 30 min, 100 μl of 1 M H_2SO_4 was added to stop the reaction followed by measured absorbance at 450 nm using Stat Fax 2100 microtiterplate reader (Awareness Technology Inc. FL, USA).

Results

DIGE and MALDI-TOF analysis of the mitochondrial proteomes across MCF-10A, MCF-7, and MDA-MB-231 cells

For mitochondrial proteome analysis, MCF-10A, MCF-7, and MDA-MB-231 were grown on cell culture dishes, and the confluency of cells was checked prior to performing mitochondrial protein extraction. To examine the efficiency of mitochondrial protein extraction, immunoblotting analysis of the LDH (lactate dehydrogenases) (cytosolic marker) and VDAC2 (mitochondrial marker) levels were carried out, and the results showed the mitochondrial fractions were significantly enriched (Fig. 1a). The 2D-DIGE analysis shows that there is a significant protein expression profiling changes between the mitochondrial fraction (Cy3/green color) and cytosolic fraction (Cy5/red color) indicating the established mitochondrial enrichment is suitable for providing downstream mitochondrial proteome analysis (Fig. 1b).

To identify altered abundance of mitochondrial proteins and relate it to the tumorigenesis of breast cancer, the mitochondrial proteomic profiles of MCF-10A, MCF-7, and MDA-MB-231 were analyzed. The three replicates of the three different mitochondrial fractions were compared by 2D-DIGE to have a global overview of breast cell tumorigenesis. After image analysis with DeCyder v7.0, more than 1,500 protein spots were well-defined (Fig. 2). In order to reduce the intrinsic variability derived from protein samples and gel-to-gel variation, only those protein spots appearing at least in all of the triplicate gel images were qualified for statistical analysis. Furthermore, biological variation analysis of spots showing greater than 1.5-fold change in expression with a *t* test score of less than 0.05 were visually checked before confirming the alterations for protein identification. Matrix-assisted laser desorption ionization–time-of-flight mass spectrometry (MALDI-TOF MS) identification revealed 125 unique differentially expressed proteins across MCF-10A, MCF-7, and MDA-MB-231 (data not shown), in which 33 (26%) identified proteins were dominantly mitochondria-located proteins. Of the 33 mitochondrial proteins, 28 and 30 of these proteins were differential expression between MCF-7/MCF-10A and

MCF7/MCF10A		MDA-MB 231/MCF10A	
Up-regulation	Down-regulation	Up-regulation	Down-regulation
Elongation factor Tu, mitochondrial	NADH dehydrogenase [ubiquinone] 1 alpha subcomplex subunit 12	Elongation factor Tu, mitochondrial	Prohibitin
Delta(3,5)-Delta(2,4)-dienoyl-CoA isomerase	NADH dehydrogenase [ubiquinone] iron-sulfur protein 3, mitochondrial / NADH-ubiquinone oxidoreductase 30 kD subunit	Succinyl-CoA:3-ketoacid-coenzyme A transferase 1 / OXCT1	Glutamate dehydrogenase 1
Pyruvate dehydrogenase E1 component subunit beta, mitochondrial	Citrate synthase	Sperm mitochondrial-associated cysteine-rich protein / MCSP	Protein ETHE1, mitochondrial / Ethylmalonic encephalopathy protein 1 / ETHE1
Sperm mitochondrial-associated cysteine-rich protein / MCSP	ATP synthase subunit d	Pyruvate dehydrogenase E1 component subunit beta, mitochondrial	Mortalin / GRP 75 / HSPA9 / Stress-70 protein, mitochondrial
Malate dehydrogenase	Glutamate dehydrogenase 1	Delta(3,5)-Delta(2,4)-dienoyl-CoA isomerase	Enoyl-CoA hydratase, mitochondrial / Enoyl-CoA hydratase 1
Ornithine aminotransferase	Cytochrome b-c1 complex subunit 2, mitochondrial / Ubiquinol-cytochrome-c reductase complex core protein 2 / Complex III subunit 2	Malate dehydrogenase	Protein HRPAP20
Cytochrome c oxidase subunit 5B, mitochondrial	Prohibitin	Cytochrome c oxidase subunit 5B, mitochondrial	NADH dehydrogenase [ubiquinone] iron-sulfur protein 3, mitochondrial / NADH-ubiquinone oxidoreductase 30 kD subunit
3-hydroxyisobutyrate dehydrogenase	HSP60	Ornithine aminotransferase	39S ribosomal protein L49
Succinyl-CoA:3-ketoacid-coenzyme A transferase 1 / OXCT1	Mortalin / GRP 75 / HSPA9 / Stress-70 protein, mitochondrial	Cytochrome c oxidase subunit VIb isoform 1	Mitochondrial inner membrane protein / Mitofilin
Calcium-binding mitochondrial carrier protein SCaMC-1	Mortalin / GRP 75 / HSPA9 / Stress-70 protein, mitochondrial	NADH dehydrogenase [ubiquinone] 1 alpha subcomplex subunit 12	Heat shock 70 kDa protein 1 / HSP70-1
39S ribosomal protein L49	Protein HRPAP20		Glycerol-3-phosphate dehydrogenase, mitochondrial
	NADH dehydrogenase [ubiquinone] iron-sulfur protein 8, mitochondrial / NADH-ubiquinone oxidoreductase 23 kD subunit		Cytochrome b-c1 complex subunit Rieske-like protein 1
	HSP60		HSP60
	Cytochrome c oxidase subunit VIb isoform 1		Cytochrome b-c1 complex subunit 2, mitochondrial / Ubiquinol-cytochrome-c reductase complex core protein 2 / Complex III subunit 2
	Cytochrome b-c1 complex subunit Rieske-like protein 1		3,2-trans-enoyl-CoA isomerase
	Protein ETHE1, mitochondrial / Ethylmalonic encephalopathy protein 1 / ETHE1		Citrate synthase
	Fumarate hydratase		ATP synthase subunit d
	Superoxide dismutase [Mn], mitochondrial		Fumarate hydratase
			Superoxide dismutase [Mn], mitochondrial
			NADH dehydrogenase [ubiquinone] iron-sulfur protein 8, mitochondrial / NADH-ubiquinone oxidoreductase 23 kD subunit

Fig. 3 Differential expressions of mitochondrial proteins across MCF-10A, MCF-7, and MDA-MB-231

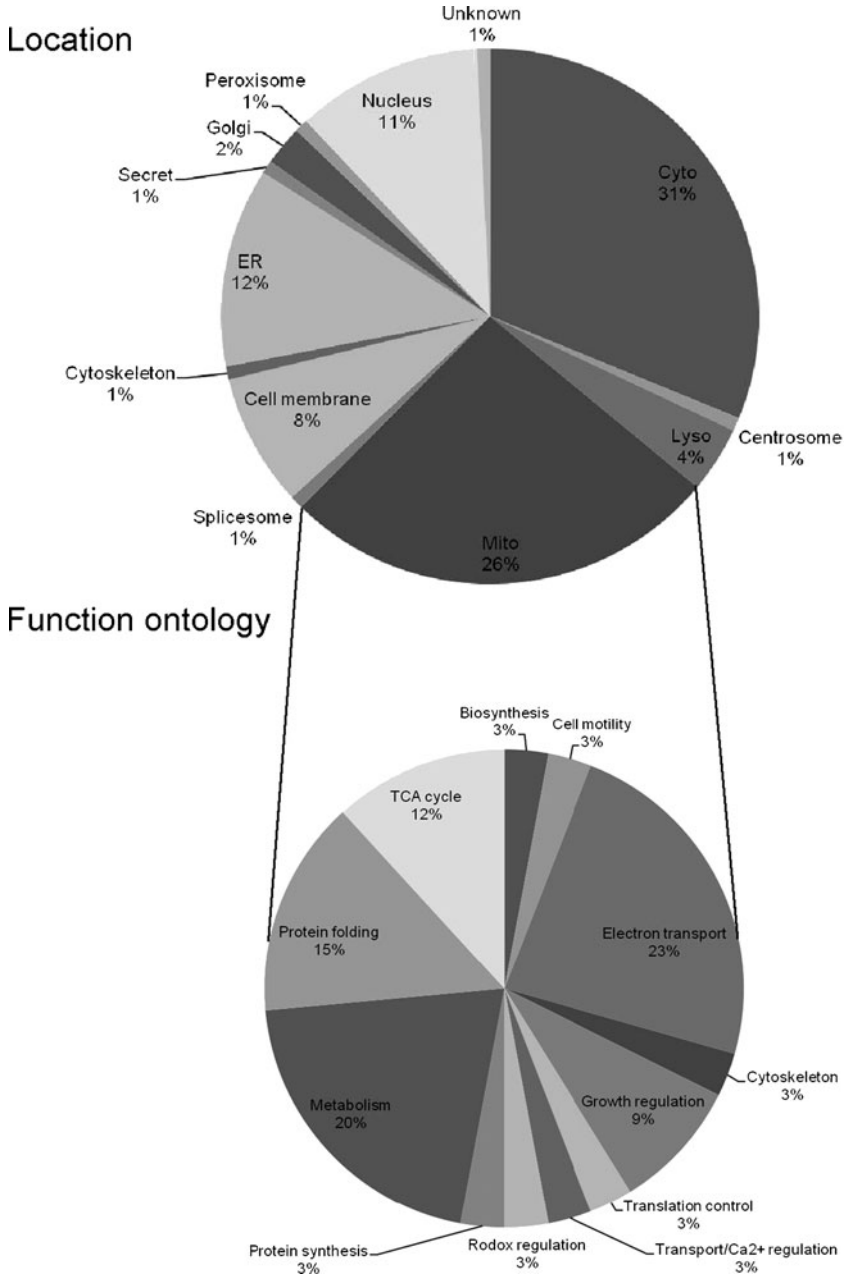

Fig. 4 Percentage of intracellular locations of isolated mitochondrial fractions identified by 2D-DIGE/MALDI-TOF MS for MCF-10A, MCF-7, and MDA-MB-231 cells (**a**). Percentage of identified mitochondrial proteins according to their biological functions (**b**)

MDA-MB-231/MCF-10A, respectively, while 20 proteins were differential expression between MDA-MB-231 and MCF-7 (Fig. 3 and Supplementary Table 1). In these mitochondrial proteins, most of them were involved in electron transport, metabolism, and protein folding (Fig. 4). Importantly, 18 and 12 out of these identified spots such as SCaMC-1 and ornithine aminotransferase have not been reported in all of cancers or breast cancer-related studies, respectively, in our knowledge means these proteins are putative mitochondrial breast cancer markers. As expect, some of well known breast cancer markers such as MnSOD, prohibitin, and mortalin were also identified in this 2D-DIGE experiment.

Validation of identified mitochondrial proteins by immunoblotting, immunofluorescence, and ELISA

Immunoblot and immunofluorescence analysis were carried out to confirm the differential protein levels observed in mitochondrial fractions across MDA-MB-231, MCF-7, and MCF-10A (Fig. 5). Both the immunoblot and immunofluorescent analysis indicated that the protein levels of MnSOD decreased in both MCF-7 and MDA-MB-231 than in MCF-10A which consist of the 2D-DIGE result shown in Fig. 3 and previous breast cancer study (Soini et al. 2001). In addition, MnSOD was primarily localized in the mitochondria, which coincided with the mitotracker-stained mitochondria (Fig. 5).

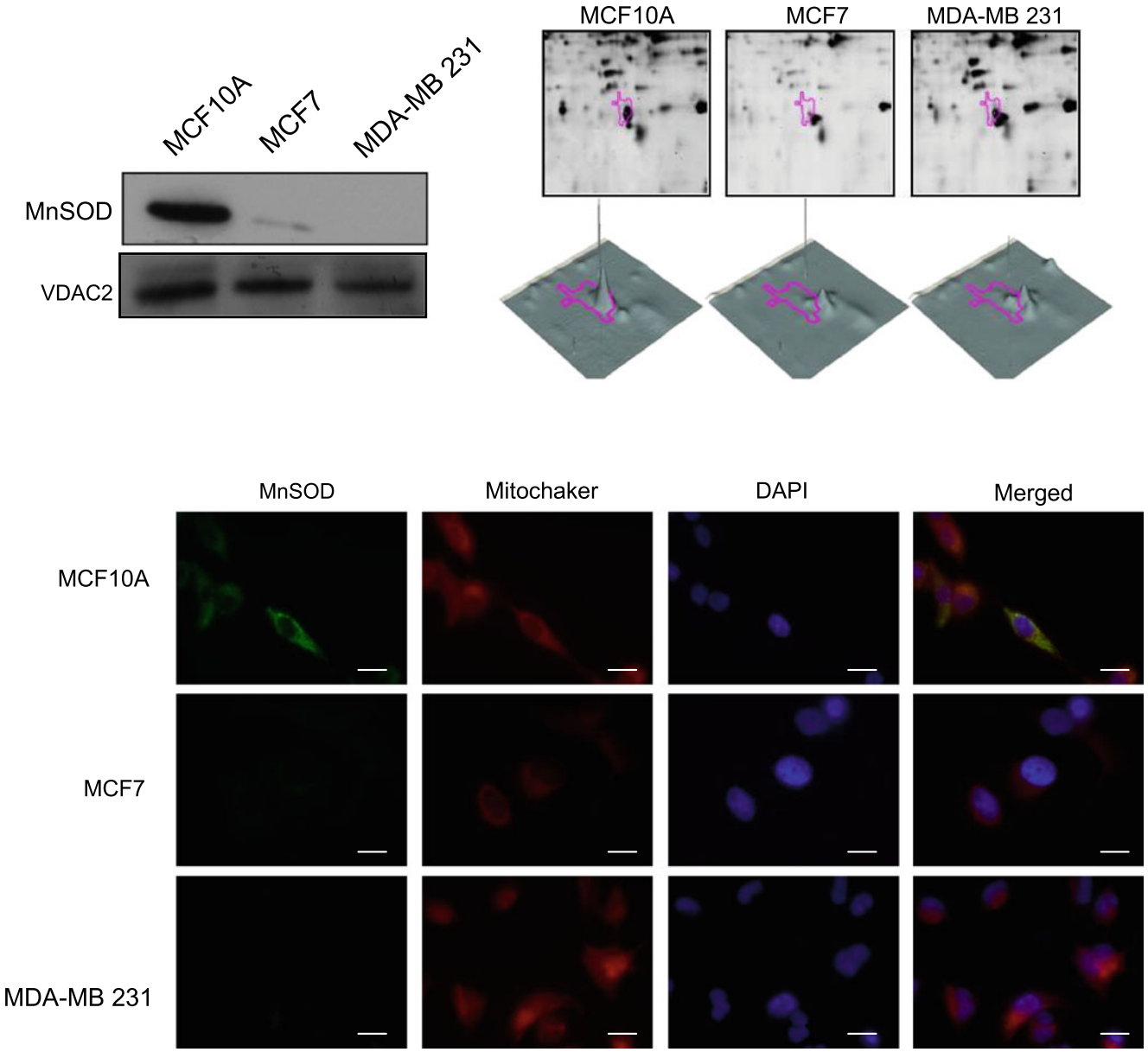

Fig. 5 Representative immunoblotting and immunofluorescence analysis for selected differentially expressed protein (MnSOD) identified by mitochondrial proteome analysis across MCF-10A, MCF-7, and MDA-MB-231 cells. Twenty micrograms of the mitochondrial lysates from breast tumor cell lines (MDA-MB-231 and MCF-7) and normal breast cell (MCF-10A) were resolved by SDS-PAGE and immunoblotted for MnSOD, while VDAC 2 was used for mitochondrial loading control (*left top panels*), 2D protein map and three-dimensional spot image (*right top panels*). A 5×10^4 MCF-10A, MCF-7, and MDA-MB-231 cells were seed on cover slips before fixation and staining for DAPI, mitotracker, and MnSOD. Each set of fields were taken using the same exposure and images are representative of six different fields. Scale bar=10 μm (*bottom panels*)

In order to further verify the protein expression levels of unreported identified proteins across MCF-10A, MCF-7, and MDA-MB-231, the expression of mitochondrial protein SCaMC-1 was examined and the immunoblotting result demonstrated that SCaMC-1 expression increased in both MCF-7 and MDA-MB-231 than in MCF-10A (Fig. 6). Additionally, the expression of SCaMC-1 in normal breast cells and a panel of breast cancer cell lines (MCF-7, MDA-MB-231, MDA-MB-453, and MDA-MB-435) were examined with immunofluorescence. The SCaMC-1 was demonstrated to be located in mitochondria due to the spatial overlapping of SCaMC-1 with mitotracker, and its expression is up-regulated in MCF-7, MDA-MB-231, MDA-MB-453, and MDA-MB-435 than in MCF-10A, implying that SCaMC-1 is overexpressed in common non-invasive and invasive breast cancer cells (Fig. 6). Further investigation of clinical plasma specimen showing that SCaMC-1 was significantly increased in breast cancer patients rather than

in the healthy donors. This increase is observed in both non-metastatic and metastatic breast cancers (Fig. 7). Thus, SCaMC-1 is potentially a candidate for breast cancer diagnosis.

Subcellular distribution of prohibitin in normal breast cells and breast cancer cells

Prohibitin, a major mitochondria-located protein, was dominantly distributed in the mitochondria of the MCF-10A cells, but was confined within the nucleus in non-invasive breast cancer cells (MCF-7 and MDA-MB-453) and in invasive breast cancer cells (MDA-MB-231, MDA-MB-361, MDA-MB-435, and SKBR3; Fig. 8). These results indicate that the prohibitin was differentially distributed between normal breast cells and breast cancer cells, and that the subcellular locations of the protein may account for tumorigenesis.

Discussion

In order to thoroughly understand the molecular mechanisms associated with tumorigenesis and metastasis, a subcellular proteomics strategy has been applied to identify the cancer markers in mitochondria that relate to tumorigenesis and metastasis (Gogvadze et al. 2008). Accordingly, we have purified mitochondrial proteins from three breast cells, MCF10A, MCF7, and MDA-MB-231, corresponding to normal luminal epithelial cells, the non-invasive breast cancer cells derived from luminal duct, and invasive breast cancer cells derived from the same tissues, respectively, followed by quantitatively identified potential mitochondrial transformation markers of breast cancer with 2D-DIGE and MALDI-TOF mass spectrometry. The experimental results demonstrate the strategy is powerful enough to identify numerous breast cancer mitochondrial signatures and offers a complementary role to LC/MS-based proteomic analysis. Even though the global coverage of protein mixtures identified by LC/MS-based analysis is generally recognized to be higher than that of 2-DE-based analysis, 2-DE-based analysis provides direct protein quantification at protein isoform levels instead of peptide levels to reduce analytical variations (Timms et al. 2008).

The results of this study show that the differentially expressed mitochondrial proteins across normal and transformed breast cell lines were enriched. Although only 26% of the isolated proteins were assigned to be mitochondria-located, the percentage is higher than the general total cellular protein analysis (~5% of total cellular proteins; Chan et al. 2005; Nagaraja et al. 2006; Lai et al. 2010). Notably, part of cytosolic proteins are able to translocate into mitochondria but are assigned to be cytosolic proteins which may contribute to the low coverage rate of the mitochondrial fractions in total enriched proteins.

Fig. 6 Immunoblotting and immunofluorescence analysis of the expression of SCaMC-1 across normal breast cell (MCF-10A) and various breast cancer cell lines (MCF-7, MDA-MB-231, MDA-MB-453, and MDA-MB-435 cells). Twenty micrograms of the mitochondrial lysates from breast tumor cell lines (MDA-MB-231 and MCF-7) and normal breast cell (MCF-10A) were resolved by SDS-PAGE and immunoblotted for calcium-binding mitochondrial carrier protein SCaMC-1, while VDAC 2 was used for mitochondrial loading control (*left top panels*), 2D protein map and three-dimensional spot image (*right top panels*). A 5×10^4 MCF-10A, MCF-7, MDA-MB-231, MDA-MB-453, and MDA-MB-435 cells were seeded on cover slips before fixation and staining for DAPI, mitotracker, and SCaMC-1. Each set of fields were taken using the same exposure and images are representative of six different fields. Scale bar=10 μm (*bottom panels*)

In previous tumorigenesis and metastasis-related breast cancer studies, Nagaraja et al. used traditional 2-DE with silver stain to reveal 26 differentially expressed proteins among transformed breast cells with different levels of invasiveness and normal cells which were the same cell lines used in the present study (Nagaraja et al. 2006). Their study showed no evidence of visualizing protein spots with sensitive strategies, and protein expression changes were not quantifiable because no broader linear-ranged methods and statistical analysis were employed. Only two out of those 26 identified proteins (cytochrome c oxidase subunit VIb and superoxide dismutase) are mitochondrial proteins, and both of these are also identified in our statistical mitochondrial 2D-DIGE data, which further evidenced the important roles of these two proteins on tumorigenesis and metastasis. Our previous report used 2D-DIGE/ MALDI-TOF to monitor the tumorigenesis and metastasis-related protein markers in total cellular proteins and extracellular secreted fractions by using the same cell model (i.e., MCF-10A, MCF-7, MDA-MB-231; Lai et al. 2010). The study has offered numerous putative breast cancer markers as well as four mitochondrial proteins (glyceraldehyde-3-phosphate dehydrogenase, superoxide dismutase, malate dehydrogenase, and prohibitin) which are coincided with our current identified mitochondrial markers. Glyceraldehyde-3-phosphate dehydrogenase and superoxide dismutase display down-regulation in both MCF-7 and MDA-MB-231 rather in MCF-10A in these two independent works. However, malate dehydrogenase is up-regulated in currently enriched MCF-7 and MDA-MB-231 mitochondrial fractions, while the protein is down-regulated in MDA-MB-231 total cell extraction. In addition, prohibitin is down-regulated in enriched MCF-7 and MDA-MB-231 mitochondrial fractions; while the protein is up-regulated in MDA-MB-231 total cell extraction. These contrasting results might be caused by the translocation of these proteins between mitochondria and other organelles. In Fig. 8, the differentially located property of prohibitin has been observed in between mitochondria and nucleus in

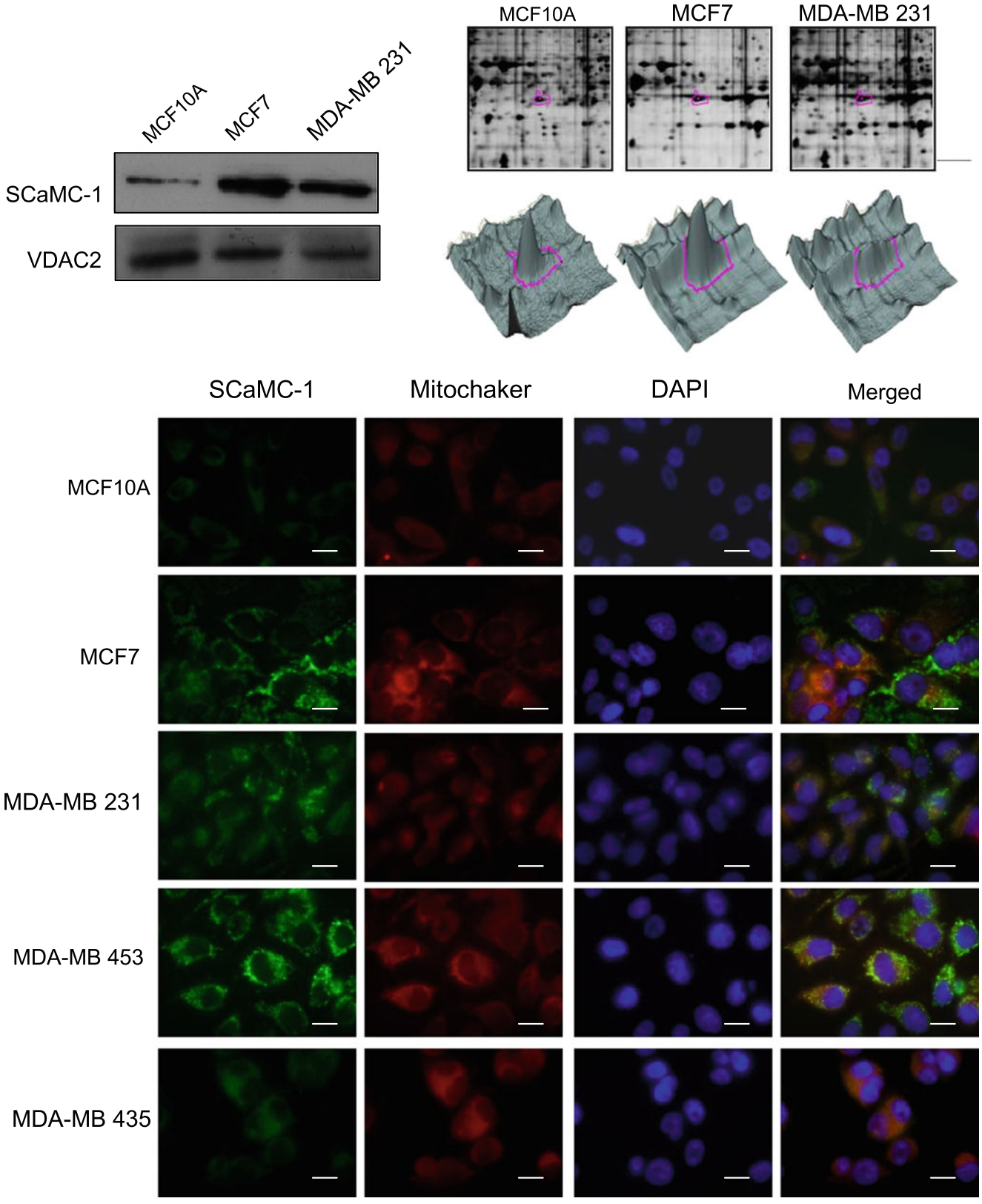
MCF10A
MCF7
MDA-MB 231
SCaMC-1
VDAC2
MCF10A
MCF7
MDA-MB 231
SCaMC-1
Mitochaker
DAPI
Merged
MCF10A
MCF7
MDA-MB 231
MDA-MB 453
MDA-MB 435

normal breast cells and in transformed breast cells, respectively. Prohibitin is originally localized in the inner mitochondrial membrane and plays a role in maintaining mitochondrial morphology (Artal-Sanz and Tavernarakis, 2009). On the other hand, some reports have also shown that prohibitin is sometimes located in the nucleus and is involved in transcriptional regulation through interacting with several transcription factors (Nijtmans et al. 2002). Until recently, Kasashima et al. reported estrogen receptor-alpha may play a key role in regulating nucleus and mitochondria shuttle of prohibitin in Hela cells (Kasashima et al. 2006). In our current study, either estrogen receptor-positive or negative breast cancer lines have seemed to perform nuclear-mitochondrial translocation suggesting mechanisms other than those involving the estrogen receptor to regulate this event.

Numerous reported breast cancer marker proteins, including cytochrome c oxidase subunit 5B, malate dehydrogenase, and elongation factor Tu which are highly expressed in both low-invasive and aggressive breast cancer cells have been identified in this study implying current proteomic strategy are potential tools for discovering breast cancer markers with reasonable reproducibility.

Importantly, several of the identified proteins such as SCaMC-1, delta(3,5)-Delta(2,4)-dienoyl-CoA isomerase, sperm mitochondrial-associated cysteine-rich protein, and succinyl-CoA:3-ketoacid-coenzyme A transferase 1 have not been reported in previous breast cancer studies, implying that these proteins need to be further investigated to confirm them as valuable breast cancer markers. Interestingly, SCaMC-1, a calcium-regulated transporter is important for calcium-sensing in mitochondria and might play role as ATP-Mg/Pi exchanger. In addition, due to the structural similarity between SCaMC-1 and calmodulin, SCaMC-1 is expected to be sensitive to calmodulin antagonists (del Arco and Satrustegui 2004). In the view of our results, our data demonstrated SCaMC-1 is significantly overexpressed in estrogen receptor-positive breast cancer cells but slightly increased in estrogen receptor negative breast cancer cells suggesting the possible interplay between estrogen receptor and SCaMC-1. Notably, plasma level of SCaMC-1 demonstrated to be significantly increased in both non-metastatic and metastatic breast cancer patients rather than in the plasma level of the healthy donors implying SCaMC-1 is a potential candidate for breast cancer diagnosis.

With the basis of a Swiss-Prot search and KEGG pathway analysis, numerous potential biological functions of the identified mitochondrial proteins across MCF-10A, MCF-7, and MDA-MB-231 were determined. Current proteomic analysis indicated mitochondrial proteins known to regulate electron transport and metabolism are found to be down-regulated and up-regulated in MCF-7, respectively. This demonstrates that cancer cells rely heavily on glycolysis instead of mitochondrial electron transport system to obtain ATP for proliferation and tumorigenesis in the presence of adequate oxygen levels (Lopez-Lazaro 2008); this mechanism has been implicated in numerous cancer therapies (Rivenzon-Segal et al. 2003; Gatenby and Gillies 2007). In addition, the expression of proteins linked to protein folding and redox-regulation decreased in both MCF-7 and MDA-MB-231 cells in comparison to the levels in MCF-10A, suggesting breast cancer cells heavily rely on glycolysis rather than mitochondrial electron transport system to obtain ATP. Consequently, less reactive oxygen species are generated and less protein modified. Thus, few proteins in response to protein folding and redox-regulation are expressed.

Deregulation of mitochondria has been reported to be one of causes in promoting tumorigenesis and metastasis via bypassing apoptotic pathways and maintaining survival signaling. Mortalin, one of the newly identified differentially expressed mitochondrial proteins across MCF-10A, MCF-7, and MDA-MB-231, is mainly a mitochondria-located protein. However, the differential distribution of mortalin in cytoplasm has been evidenced to significantly contribute to tumorigenesis (Wadhwa et al. 1993b). Over-expression of mortalin in cytosol appears not only to sequester the tumor suppressor protein p53, but also to activate the oncogenic *Ras–Raf* signaling pathway, subsequently promotes cell cycle progression and interferes with apoptotic pathway that lead to a net result of tumor growth (Wadhwa et al. 2002b;Wadhwa et al. 2003b). In our study, the down-regulation of mitochondrial mortalin in breast cancer cells possibly reflects the increase of mortalin in cytosol, implying the promotion of cell cycle progression, tumorigenesis, and metastasis. Succinyl-CoA/3-ketoacid-coenzyme A transferase 1 is a key enzyme in the metabolism of monoacetoacetin. This enzyme has shown to promote tumorigenesis via inhibiting apoptosis at multiple points in the apoptotic signaling pathway in

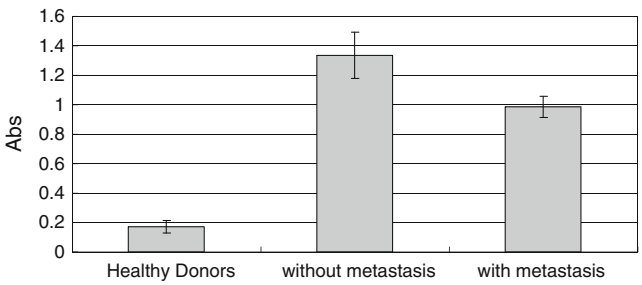

Fig. 7 ELISA analysis of plasma SCaMC-1 levels in healthy donors, breast cancer patients without metastasis, and breast cancer patients with metastasis. Plasma samples were obtained from five healthy individuals, five breast cancer patients without detectable metastasis, and five breast cancer patients presenting metastasis at the time of serum collection. Fifty micrograms of plasma samples were coated onto each well of 96-well plate for ELISA analysis and the absorbance was measured at 450 nm using Stat Fax 2100 microtiterplate reader

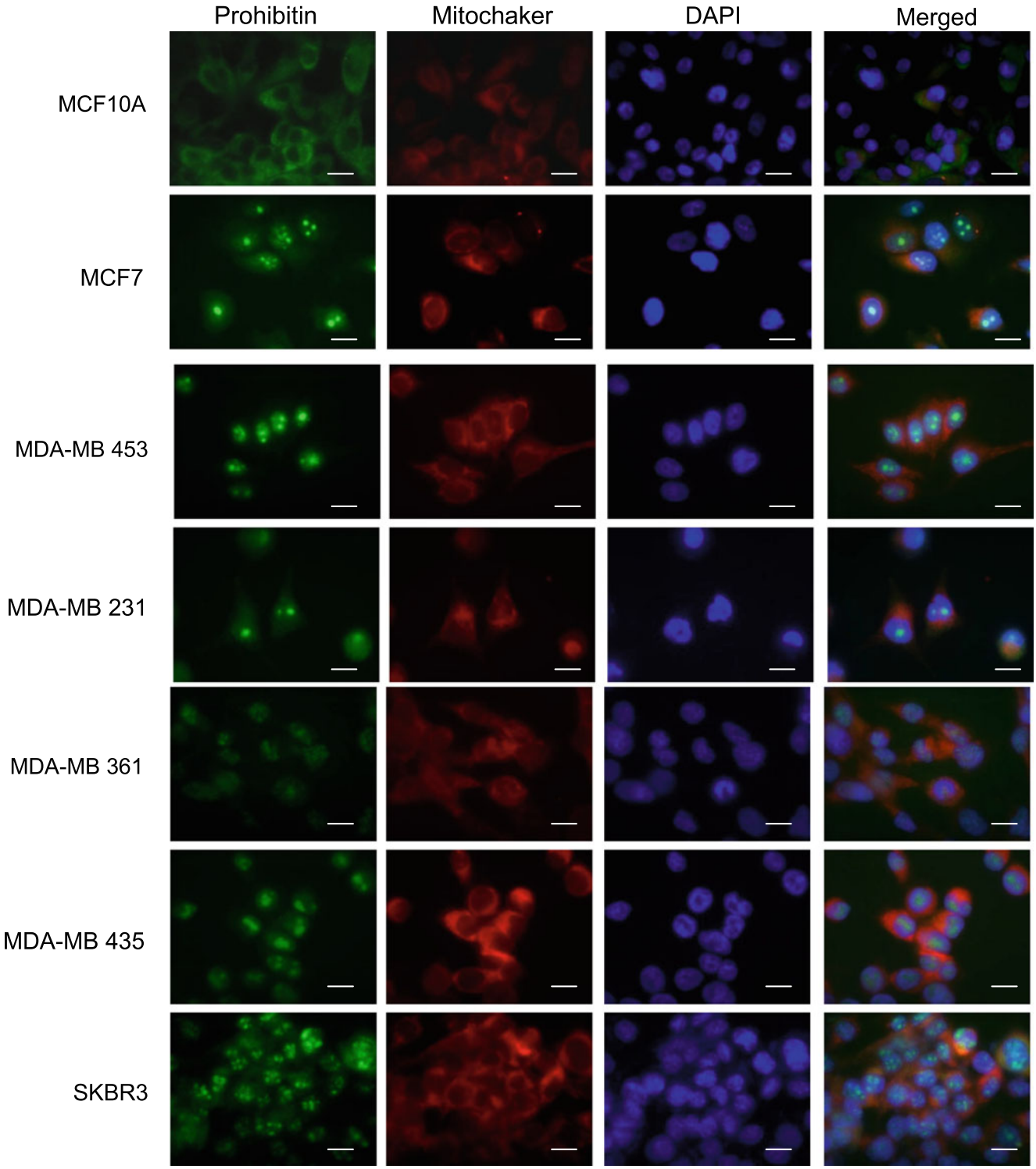

Fig. 8 Immunofluorescence analysis of subcellular distribution of prohibitin across MCF-10A, MCF-7, MDA-MB-453, MDA-MB-231, MDA-MB-361, MDA-MB-435, and SKBR3 cells. MCF-10A, MCF-7, MDA-MB-453, MDA-MB-231, MDA-MB-361, MDA-MB-435, and SKBR3 cells on cover slips were fixed and stained with prohibitin, mitotracker, and DAPI. Each set of fields were taken using the same exposure, and images are representative of six different fields. Scale bar=10 μm

human hepatocarcinoma (Feng et al. 2007). Additionally, Succinyl-CoA/3-ketoacid-coenzyme A transferase 1 has been proved to play a growth-promoting role in human gastric cancer cells (Sawai et al. 2004). Thus, our data show the overexpression of succinyl-CoA: 3-ketoacid-coenzyme A transferase 1 in MCF-7 and MDA-MB-231 cells is correlated with the progress of tumorigenesis as well as metastasis (supplementary Table 1).

Although mitochondria contain their own DNA, ribosomes, and other machinery for protein synthesis, most mitochondrial proteins are encoded in the cell nucleus and imported from the cytosol. Accordingly, numerous chromosome-encoded proteins have been identified in our current mitochondrial proteomics analysis, in which ornithine aminotransferase and succinyl-CoA/3-ketoacid-coenzyme A transferase 1 have been found to be overexpressed in transformed cells in their transcription levels. Ornithine aminotransferase followed by suppression subtractive hybridization analysis has been evidenced to be overexpressed in human hepatocellular carcinoma in comparison with the adjacent non-tumor liver tissue (Miyasaka et al. 2001). Gene expression of succinyl-CoA/3-ketoacid-coenzyme A transferase 1 has been identified to be up-regulated in associated with overexpressed HER-2/neu gene in human breast cancer cells (MCF-7) and is known to involve in metabolic pathways of more rapidly growing cells (Oh et al. 1999). Thus, the enhancements of these two proteins in mitochondrial proteomics during tumor formation are probably contributed by the overexpressed genes of these two proteins in nucleus.

In summary, a comprehensive proteomic strategy for mitochondrial cancer marker discovery was established in this study. By using 2D-DIGE and MALDI-TOF MS, we have presented in this study a set of candidate mitochondrial protein markers that can serve as cancer markers for breast tumorigenesis and invasiveness. Moreover, some of these markers such as SCaMC-1 may be potential enough to develop as diagnostic and therapeutic candidates. Furthermore, mitochondrial protein prohibitin has shown to be differentially distributed in between normal breast cells and breast cancer cell which might account for the formation of tumorigenesis and metastasis.

Acknowledgments This work was supported by grant (NSC 99-2311-B-007-002) from the National Science Council, Taiwan, NTHU Booster grant (99N2908E1) from the National Tsing Hua University, and grant (VGHUST99-P5-22) Veteran General Hospitals University System of Taiwan.

References

Artal-Sanz M, Tavernarakis N (2009) Prohibitin and mitochondrial biology. Trends Endocrinol Metab 20:394–401

Chan HL, Gaffney PR, Waterfield MD, Anderle H, Peter MH, Schwarz HP, Turecek PL, Timms JF (2006) Proteomic analysis of UVC irradiation-induced damage of plasma proteins: serum amyloid P component as a major target of photolysis. FEBS Lett 580:3229–3236

Chan HL, Gharbi S, Gaffney PR, Cramer R, Waterfield MD, Timms JF (2005) Proteomic analysis of redox- and ErbB2-dependent changes in mammary luminal epithelial cells using cysteine- and lysine-labelling two-dimensional difference gel electrophoresis. Proteomics 5:2908–2926

Chandel NS, McClintock DS, Feliciano CE, Wood TM, Melendez JA, Rodriguez AM, Schumacker PT (2000) Reactive oxygen species generated at mitochondrial complex III stabilize hypoxia-inducible factor-1alpha during hypoxia: a mechanism of O2 sensing. J Biol Chem 275:25130–25138

Chi SL, Wahl ML, Mowery YM, Shan S, Mukhopadhyay S, Hilderbrand SC, Kenan DJ, Lipes BD, Johnson CE, Marusich MF, Capaldi RA, Dewhirst MW, Pizzo SV (2007) Angiostatin-like activity of a monoclonal antibody to the catalytic subunit of F1F0 ATP synthase. Cancer Res 67:4716–4724

Chou HC, Chen YW, Lee TR, Wu FS, Chan HT, Lyu PC, Timms JF, Chan HL (2010) Proteomics study of oxidative stress and Src kinase inhibition in H9C2 cardiomyocytes: a cell model of heart ischemia reperfusion injury and treatment. Free Radic Biol Med 49:96–108

del Arco A, Satrustegui J (2004) Identification of a novel human subfamily of mitochondrial carriers with calcium-binding domains. J Biol Chem 279:24701–24713

Esteban MA, Tran MG, Harten SK, Hill P, Castellanos MC, Chandra A, Raval R, O'brien TS, Maxwell PH (2006) Regulation of E-cadherin expression by VHL and hypoxia-inducible factor. Cancer Res 66:3567–3575

Feng Y, Tian ZM, Wan MX, Zheng ZB (2007) Protein profile of human hepatocarcinoma cell line SMMC-7721: identification and functional analysis. World J Gastroenterol 13:2608–2614

Gatenby RA, Gillies RJ (2007) Glycolysis in cancer: a potential target for therapy. Int J Biochem Cell Biol 39:1358–1366

Gharbi S, Gaffney P, Yang A, Zvelebil MJ, Cramer R, Waterfield MD, Timms JF (2002) Evaluation of two-dimensional differential gel electrophoresis for proteomic expression analysis of a model breast cancer cell system. Mol Cell Proteomics 1:91–8

Gogvadze V, Orrenius S, Zhivotovsky B (2008) Mitochondria in cancer cells: what is so special about them? Trends Cell Biol 18:165–173

Hondermarck H, Dolle L, Yazidi-Belkoura I, Vercoutter-Edouart AS, Adriaenssens E, Lemoine J (2002) Functional proteomics of breast cancer for signal pathway profiling and target discovery. J Mammary Gland Biol Neoplasia 7:395–405

Huang HL, Hsing HW, Lai TC, Chen YW, Lee TR, Chan HT, Lyu PC, Wu CL, Lu YC, Lin ST, Lin CW, Lai CH, Chang HT, Chou HC, Chan HL (2010) Trypsin-induced proteome alteration during cell subculture in mammalian cells. J Biomed Sci 17:36

Kasashima K, Ohta E, Kagawa Y, Endo H (2006) Mitochondrial functions and estrogen receptor-dependent nuclear translocation of pleiotropic human prohibitin 2. J Biol Chem 281:36401–36410

Kulasingam V, Diamandis EP (2007) Proteomics analysis of conditioned media from three breast cancer cell lines: a mine for biomarkers and therapeutic targets. Mol Cell Proteomics 6:1997–2011

Kumar B, Koul S, Khandrika L, Meacham RB, Koul HK (2008) Oxidative stress is inherent in prostate cancer cells and is required for aggressive phenotype. Cancer Res 68:1777–1785

Lai TC, Chou HC, Chen YW, Lee TR, Chan HT, Shen HH, Lee WT, Lin ST, Lu YC, Wu CL, Chan HL (2010) Secretomic and proteomic analysis of potential breast cancer markers by two-dimensional differential gel electrophoresis. J Proteome Res 9:1302–1322

Lee WY, Huang SC, Tzeng CC, Chang TL, Hsu KF (2007) Alterations of metastasis-related genes identified using an oligonucleotide microarray of genistein-treated HCC1395 breast cancer cells. Nutr Cancer 58:239–246

Lopez-Lazaro M (2008) The warburg effect: why and how do cancer cells activate glycolysis in the presence of oxygen? *Anticancer Agents Med*. Chem 8:305–312

Miyasaka Y, Enomoto N, Nagayama K, Izumi N, Marumo F, Watanabe M, Sato C (2001) Analysis of differentially expressed

genes in human hepatocellular carcinoma using suppression subtractive hybridization. Br J Cancer 85:228–234

Morrow T (2007) Gene expression microarray improves prediction of breast cancer outcomes. Manag Care 16:51–52

Nagaraja GM, Othman M, Fox BP, Alsaber R, Pellegrino CM, Zeng Y, Khanna R, Tamburini P, Swaroop A, Kandpal RP (2006) Gene expression signatures and biomarkers of noninvasive and invasive breast cancer cells: comprehensive profiles by representational difference analysis, microarrays and proteomics. Oncogene 25:2328–2338

Nijtmans LG, Artal SM, Grivell LA, Coates PJ (2002) The mitochondrial PHB complex: roles in mitochondrial respiratory complex assembly, ageing and degenerative disease. Cell Mol Life Sci 59:143–155

Nuyten DS, van de Vijver MJ (2008) Using microarray analysis as a prognostic and predictive tool in oncology: focus on breast cancer and normal tissue toxicity. Semin Radiat Oncol 18:105–114

Oh JJ, Grosshans DR, Wong SG, Slamon DJ (1999) Identification of differentially expressed genes associated with HER-2/neu overexpression in human breast cancer cells. Nucleic Acids Res 27:4008–4017

Pouyssegur J, Dayan F, Mazure NM (2006) Hypoxia signalling in cancer and approaches to enforce tumour regression. Nature 441:437–443

Pucci-Minafra I, Fontana S, Cancemi P, Alaimo G, Minafra S (2002) Proteomic patterns of cultured breast cancer cells and epithelial mammary cells. Ann NY Acad Sci 963:122–139

Rivenzon-Segal D, Boldin-Adamsky S, Seger D, Seger R, Degani H (2003) Glycolysis and glucose transporter 1 as markers of response to hormonal therapy in breast cancer. Int J Cancer 107:177–182

Sawai M, Yashiro M, Nishiguchi Y, Ohira M, Hirakawa K (2004) Growth-inhibitory effects of the ketone body, monoacetoacetin, on human gastric cancer cells with succinyl-CoA: 3-oxoacid CoA-transferase (SCOT) deficiency. Anticancer Res 24:2213–2217

Soini Y, Vakkala M, Kahlos K, Paakko P, Kinnula V (2001) MnSOD expression is less frequent in tumour cells of invasive breast carcinomas than in in situ carcinomas or non-neoplastic breast epithelial cells. J Pathol 195:156–162

Taylor RW, Turnbull DM (2005) Mitochondrial DNA mutations in human disease. Nat Rev Genet 6:389–402

Timms JF, Cramer R (2008) Difference gel electrophoresis. Proteomics 8:4886–4897

von Jagow G, Engel WD (1980) Structure and function of the energy-converting system of mitochondria. Angew Chem Int Ed Engl 19:659–675

Wadhwa R, Kaul SC, Sugimoto Y, Mitsui Y (1993) Spontaneous immortalization of mouse fibroblasts involves structural changes in senescence inducing protein, mortalin. Biochem Biophys Res Commun 197:202–206

Wadhwa R, Yaguchi T, Hasan MK, Mitsui Y, Reddel RR, Kaul SC (2002) Hsp70 family member, mot-2/mthsp70/GRP75, binds to the cytoplasmic sequestration domain of the p53 protein. Exp Cell Res 274:246–253

Wadhwa R, Yaguchi T, Hasan MK, Taira K, Kaul SC (2003) Mortalin-MPD (mevalonate pyrophosphate decarboxylase) interactions and their role in control of cellular proliferation. Biochem Biophys Res Commun 302:735–742